Accountable Textual-Visual Chat Learns to Reject Human Instructions in Image Re-creation

Anonymous authors
Paper under double-blind review

Abstract

The recent success of ChatGPT and GPT-4 has drawn widespread attention to multimodal dialogue systems. However, there is a lack of datasets in the academic community that can effectively evaluate the multimodal generation capabilities of Visual Language Models (VLMs) in textual-visual chat tasks. In this paper, we address this gap by introducing two novel multimodal datasets: the synthetic CLEVR-ATVC dataset (620K) and the manually pictured Fruit-ATVC dataset (50K). These datasets incorporate both visual and text-based inputs and outputs. Furthermore, to facilitate the accountability of multimodal systems in rejecting human requests, similar to language-based ChatGPT conversations, we introduce specific rules as supervisory signals within the datasets. This allows the trained VLM to provide a yes or no answer after engaging in visual and textual reasoning, accompanied by a language explanation to clarify the reasons behind the inability to execute the given human instruction. Our proposed method involves a two-stage training procedure, which includes training the image auto-encoder and the auto-regressive transformer from scratch. The first stage employs a discrete variational autoencoder (dVAE) to compress each image into concise tokens, which are then combined with text tokens into a single data stream. This stream is subsequently fed into the decoder-based transformer to generate visual re-creations and textual feedback in the second stage. We conduct comprehensive analyses of experimental results, focusing on re-created image quality, answer accuracy, and the model's behavior when faced with uncertainty and imperfect user queries. Through our explorations and findings, we aim to contribute valuable insights into the accountability of textual-visual generative models.

1 Introduction

Recently, the most important breakthrough was made by ChatGPT OpenAI (2023a) and GPT-4 OpenAI (2023b), which unveiled the emerging potential of the conversation between human and artificial intelligence system. ChatGPT serves as a chatbot that operates with language as both input and output, while GPT-4 is a multimodal model capable of accepting both image and text inputs and producing text outputs. A successful multimodal generative model should excel in both textual and visual reasoning, generating high-quality text and image feedback. Visual ChatGPT Chenfei Wu & Duan (2023) is a pioneering work that combines ChatGPT with a series of pre-trained visual foundation models, enabling text-image chat. Another relevant work, FROMAGe Jing Yu Koh (2023), also involves image-text inputs and outputs for multimodal dialogue, with the fine-tuning of linear layers and the freezing of pre-trained LLM. However, existing datasets lack definitive ground truths to effectively measure the quality of text and images generated in multimodal dialogue systems. Therefore, there is an urgent need for a dataset that can evaluate the performance of multimodal generative models. In this paper, we aim to address this need by constructing new multimodal datasets that require models to output high-quality images and provide textual feedback while accepting a text-image pair. We introduce the synthetic CLEVR-ATVC dataset (620K), created by rendering images using approximately 200 GPU days, and the real Fruit-ATVC dataset (50K), manually captured and annotated.

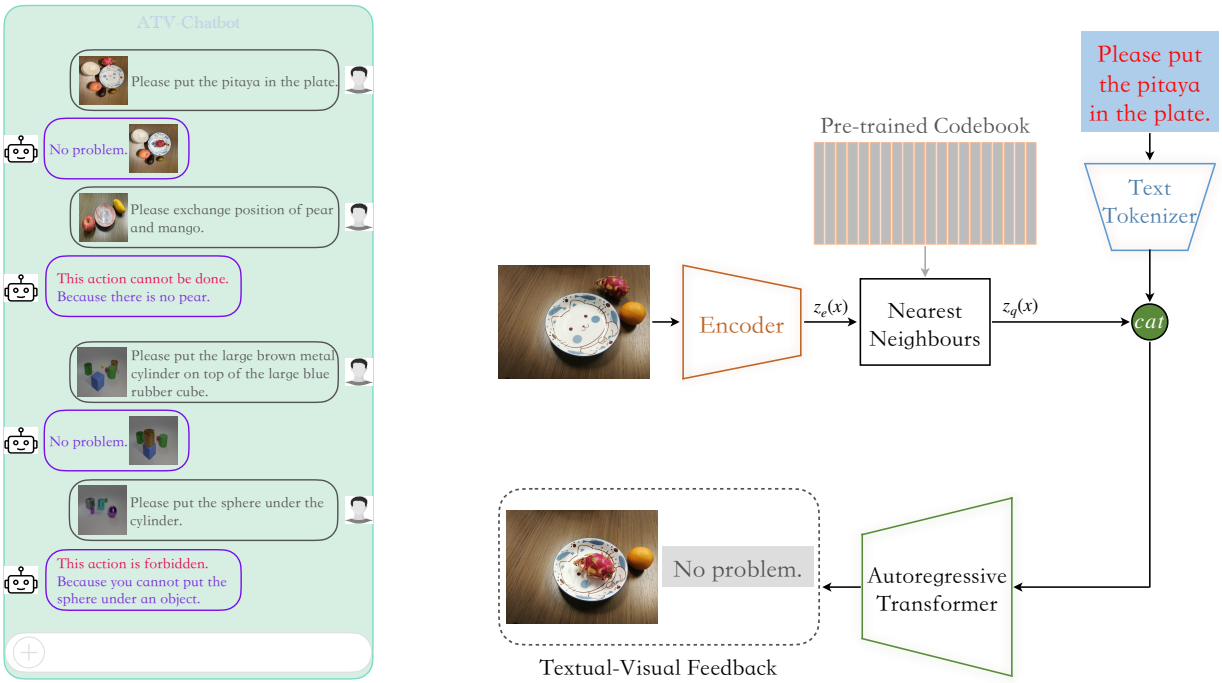

Figure 1: The left figure shows that a multimodal generative model can simultaneously recreate visual input and give textual feedback when faced with human instructions, especially it can reject some commands. The right figure illustrates the overall framework of our method. The model is required to generate a re-created image (**M**) and a textual feedback (**A**) conditioned on the visual input (**V**) and text-based user query (**T**), and the language-based explanation is also given for those instructions that cannot be executed and the prohibited instructions.

Another significant contribution of this paper pertains to the issue of responsibility in text-to-image generation models, specifically the need for models to learn how to reject human instructions. Previous works Doshi-Velez et al. (2017); Loi & Spielkamp (2021) have highlighted the importance of accountability in AI systems, including the ability to hold decision-makers accountable for adhering to procedural and substantive standards. The responsible management and deployment of AI systems is a crucial and often overlooked topic. ChatGPT OpenAI (2023a) implements a similar requirement at deployment time by employing rules defined by OpenAI to restrict certain requests. However, to the best of our knowledge, we are the first to consider the issue of responsibility in textual-visual dialogue models. Previous text-to-image generation methods Ramesh et al. (2021a); Nichol et al. (2021); Wu et al. (2021); Ramesh et al. (2022); Saharia et al. (2022); Ding et al. (2021) have produced random and uncontrolled outcomes lacking human oversight. While some works have explored the controllability of image generation by focusing on object categories or attributes (e.g., position, pose, color) Li et al. (2019); Niemeyer & Geiger (2021); Jiang et al. (2022); Patashnik et al. (2021), such as StyleCLIP Patashnik et al. (2021), which manipulates visual image attributes using text, the rejection of human instructions and providing explanations for such decisions have not been adequately addressed in the textual-visual dialogue context. Therefore, in this paper, we propose that the machine should be capable of rejecting human instructions and providing explanations, particularly for instructions that cannot be executed or are prohibited.

To serve the aforementioned research goals, we introduce a novel task called accountable text-based visual re-creation, which explores whether textual-visual chat models can learn to reject human instructions. This task requires the model to generate both visual re-creations and language-based feedback while accepting a text-image pair. Our datasets include rules as supervision signals to teach the model to reject certain instructions. As illustrated in Figure 1, when a chatbot receives instructions from a human, it responds with a "no" to forbidden or unfeasible instructions, accompanied by an explanation. An instruction may

be deemed unfeasible if the corresponding objects mentioned in the text-based query are absent in the visual input. Prohibited instructions are determined manually, taking into account the laws of physics. These instructions are further elaborated and listed in Table 3. Our proposed method, as depicted in Figure 1, employs a multimodal generative model comprising an image auto-encoder and an auto-regressive transformer. We propose a two-stage training procedure to train these components from scratch. The first stage involves a discrete variational autoencoder (dVAE) that compresses each image into concise tokens, which are then concatenated with text tokens and fed into the decoder-based transformer responsible for generating the visual re-creations and textual feedback.

Additionally, we provide comprehensive analysis of our experimental results, including assessments of re-created image quality, answer accuracy, and the model's behavior when faced with uncertainty and imperfect user queries. We also compare two different image auto-encoders, VQVAE Oord et al. (2017) and VQGAN Esser et al. (2021), and analyze the reasons behind the subpar performance of VQGAN. All the datasets used in this study are publicly available for non-commercial use, and we will release the source code for our annotation tool, evaluation tool, implementation of baseline models, metric calculations, and detailed instructions.

To summarize, the main contributions of this paper are as follows:

- We construct two multimodal datasets, CLEVR-ATVC (620K) and Fruit-ATVC (50K), which incorporate visual and textual inputs and outputs to evaluate the performance of multimodal generative models.
- We consider the issue of accountability in multimodal generative models by embedding pre-set rules as supervised signals in our datasets. This enables the VLMs to learn to reject human instructions in multimodal conversations.
- We propose a two-stage training procedure for training the image auto-encoder and auto-regressive transformer, aiming to enable the models to learn how to reject human instructions. All of our models are trained from scratch, and their training took 350∼900 GPU days on our constructed datasets.
- We provide extensive qualitative and quantitative results, evaluating the quality of generated images, the accuracy of answers, and the model's ability to handle uncertainty and incomplete queries.

The remainder of this paper is organized as follows. Section 2 presents detailed information about our datasets. In Section 3, we introduce our models and training process. We then present extensive experiments and detailed analysis in Section 4 to validate our proposed method. Section 5 provides an overview of related work, and Section 6 concludes the paper. Additional details of our datasets are provided in the appendix.

2 Datasets

In this section, we present the distinctive aspects of our datasets compared to existing ones. We then describe the data collection process. Additionally, we provide an overview of the information contained in the annotation files for our datasets, with more detailed information available in the appendix. Finally, we summarize the dataset statistics in the tables.

2.1 Definition of ATVC

Our proposed dataset and task introduce two key innovations compared to previous methods. Firstly, our multimodal dataset comprises image-text inputs and outputs, which facilitates the development of more effective multimodal generative models. Secondly, our datasets incorporate predefined rules that teach the model to reject certain human instructions, even if they are technically feasible. This gives rise to the concept of accountable text-based visual re-creation (ATVC) task, which can be defined as follows:

Given a visual input ($\mathbf{V}$) and a text-based query ($\mathbf{T}$), the multimodal generative model is expected to produce a re-created image ($\mathbf{M}$) and provide a language-based explanation ($\mathbf{A}$) for its decisions. A successful ATVC

Table 1: The summary information of CLEVR-ATVC dataset.

CLEVR-ATVC					
Size	Train Pairs	Test size	Textual-Visual Feedback	Data type	
68 GB	619,741	5,000	Yes	Synthetic	
Please <action1> {size color material} [object] <action1> {size color material} [object].					
Please <action2> of {size color material} [object] and {size color material} [object].					
Action1	Action2	Size	Color	Material	Object
put on top	exchange color	big	red, green, blue, cyan	metal	cylinder
put under	exchange position	small	purple, brown, yellow	rubber	cube, sphere

Table 2: The summary information of Fruit-ATVC dataset.

Fruit-ATVC					
Size	Train Pairs	Test size	Textual-Visual Feedback	Data type	
168 GB	27,503	1,872	Yes	Real	
Please <action1> [object].					
Please <action2> of [object] and [object].					
Please <action3> [object] <action3> [container].					
Action1	Action2	Action3	Object	Container	
remove	exchange position	put in	apple, coconut, lemon etc.	plate, bottle, etc.	

model should possess the ability to comprehend the user's query and employ language cues to reason about the visual input, while also generating appropriate textual feedback and re-created visual results.

2.2 Data Collection

In order to validate the proposal of this paper, we conduct experiments on two distinct datasets. The first dataset, CLEVR-ATVC, is a large-scale synthetic dataset specifically designed to comprehensively evaluate the proposed task. On the other hand, the Fruit-ATVC dataset is utilized to evaluate our method on real-world scenarios. In the following sections, we provide a detailed description of the visual image collection process for both datasets.

CLEVR-ATVC: We utilize the default environmental settings, including object settings and rendering options, from CLEVR Liu et al. (2019) to generate synthetic images. The rendered images have a size of 256, with each image containing 3 to 6 objects. In addition, we apply a desiged algorithmic filter to exclude scenes with objects located on the image border before rendering. This ensures that all objects in both the original and re-created images are within the boundaries, facilitating the evaluation of experimental results. The synthetic CLEVR-ATVC dataset is generated over approximately 200 GPU days.

Fruit-ATVC: This dataset consists of real-world scenarios where all the images are captured manually by the authors using mobile phones and tripods. The images are taken with various mobile phone models, including iPhone, Huawei, Xiaomi, and others. For the Fruit-ATVC dataset, five researchers contributed to capturing the visual inputs and re-created images. Additionally, we incorporated 12 different scenes to enhance the diversity of the dataset. The diversity of collection scenes is illustrated in the figures provided in the appendix.

2.3 Generation of Textual Query and Feedback

For the CLEVR-ATVC dataset, we employ an automated program that simultaneously generates visual inputs, text-based queries, re-created images, and textual feedbacks. This program saves the visual inputs and re-created images in their respective folders, while the text-based queries, textual feedbacks, and other

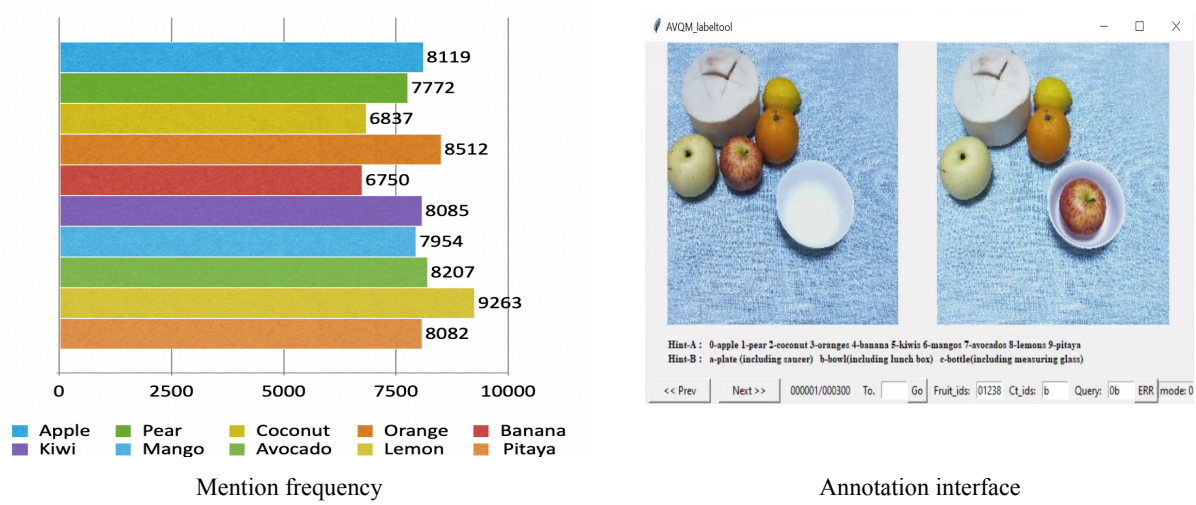

Figure 2: The mention frequency of different fruits and the annotation interface for Fruit-ATVC dataset.

Table 3: The detailed information of textual feedback.

Textual Feedback		
Answer Type	Reason for prohibition	Explanation
1) No problem.	/	/
2) Cannot be done.	/	no mentioned objects
3) Forbidden.	cannot put certain object under an object	no mentioned objects
4) Forbidden.	cannot put an object on top of certain object	no mentioned objects

data information are automatically stored in an annotation file. Each visual input is associated with ten different text-based queries and their corresponding textual feedbacks. Among these queries, six instructions can be executed by the AI system, resulting in appropriate image re-creations, while two instructions cannot be executed due to the presence of objects mentioned in the text-based queries that are not present in the visual input. Additionally, two instructions are deliberately prohibited by manual specification.

The process of generating text-based queries and textual feedbacks for the Fruit-ATVC dataset differs from the aforementioned process. Since the visual inputs and re-created images are manually captured, and the text-based queries and textual feedbacks are generated semi-automatically using our designed labeling tool. Initially, we collect and organize the visual inputs and re-created images according to predefined rules, ensuring the inclusion of executable and non-executable queries for each visual input. Then, we utilize an annotation interface (illustrated in Figure 2) to assist in generating text-based queries and textual feedbacks, which are automatically saved to an annotation file. The specific process is as follows: we select image pairs consisting of the visual input and the re-created image for executable instructions. These image pairs are then imported automatically through the interface depicted in Figure 2, where the object ID, container ID, and query type are manually added to the designated fields on the interface ("fruit_ids", "Ct_ids", and "Query", respectively). The "fruit_ids" field includes all the fruit types depicted in the image, while the "Query" field is filled with the object and container categories involved in the operation. For instance, "0b" represents an apple and a bowl. Finally, by pressing the "ERR" key, text queries and feedback are automatically generated.

2.4 Data Annotation

In this section, we present the structure of our data annotation file, which follows the format of the COCO dataset Lin et al. (2014). The main format, depicted in Figure 2.4, consists of four parts: text-based query (T), visual input (V), re-created image (M), and textual feedback (A). Since each visual input corresponds

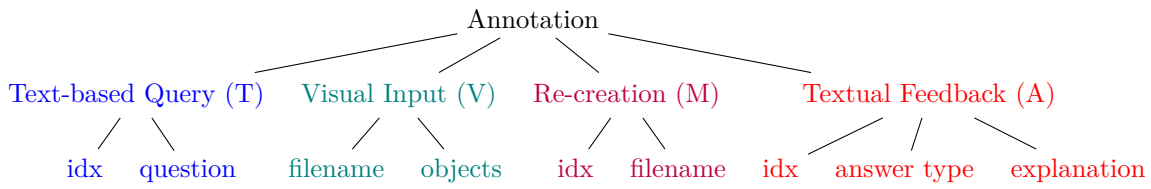

Figure 3: The main format visualization of data annotation file. The details can be found in the appendix.

to multiple text-based queries, we utilize an "idx" value to establish a one-to-one mapping between T, M, and A. The "objects" subkey enumerates the objects present in the visual input. The "explanation" provides a rationale for prohibition and explains the absence of certain objects. Table 3 provides further details on the textual feedback. There are three types of answers: a) no problem; b) the action cannot be performed; and c) the action is prohibited. Two specific instructions are prohibited: placing a certain object under another object and placing an object on top of a certain object. The prohibited actions include those that can be performed and those that cannot be performed. For prohibited instructions that cannot be executed, the model needs to provide further explanations. Please refer to the example given in Table 4. In addition, the results in Table 6 show that we conducted statistics on accuracy of answer type and accuracy of explanation in textual feedback.

2.5 Data Statistics

Table 1 and Table 2 present the summarized information of our constructed datasets.

CLEVR-ATVC consists of a training set with a total of 620,000 pairs and a testing set with 500 visual inputs, each accompanied by 10 queries, resulting in a total of 5,000 pairs. This dataset incorporates four action types: "exchange color", "exchange position", "put under", and "put on top". The rendered images encompass three object shapes, seven object colors, two object materials, and other attributes, leading to hundreds of millions of possible combinations. The text-based queries follow two different templates: the first template is used for "put on top" and "put under" actions, while the second template is employed for "exchange color" and "exchange position" actions.

Fruit-ATVC comprises 27,503 training pairs and 1,872 pairs in the testing set. This dataset involves ten different types of fruits, namely apple, pear, coconut, orange, banana, kiwi, mango, avocado, lemon, and pitaya. The frequency of mentions for each fruit is depicted in Figure 2. Additionally, the dataset includes 14 types of containers. Regarding the queries, there are three types of actions: "put a fruit in a container", "exchange positions of the fruits", and "remove the container".

3 Method

In our method, the generative model includes an image auto-encoder and an auto-regressive transformer Vaswani et al. (2017) to predict tokens of re-created image and textual feedback. The framework of our method is shown in Figure 1. Our method is a two-stage training procedure, similar to Ramesh et al. (2021a).

Image Auto-encoder This stage forces the model to learn the sequential discretized latent space of high dimensional images to utilize the expressive transformer architecture, *i.e.*, learning a codebook to encode the visual input. Given an image of resolution 256×256, a quantization model encodes it into $32 \times 32 = 1024$ discretized latent codes where the codebook size is 8192. We have tried two alternatives, including Vector Quantized Variational Autoencoder (VQVAE) Oord et al. (2017) and VQGAN Esser et al. (2021). As illustrated in Figure 1, the VQVAE can learn a latent space matrix with discrete learnable variables, which is trained end-to-end via straight-through estimation. The codebook and the VQVAE model can be trained

end-to-end using the following objective:

$$\mathcal{L}_{VQ}(G,C,E) = \underbrace{\|sg[E(v)]-e\|_2^2}_{\mathcal{L}_{codebook}} + \underbrace{\beta\,\|sg[e]-E(v)\|_2^2}_{\mathcal{L}_{commit}} + \underbrace{\|v-G(e)\|_2^2}_{\mathcal{L}_{rec}}, \tag{1}$$

where v is the visual input, e is the embedding for learning the codebook-indices, C is the learned codebook, E is the image encoder, $G(e)$ is the decoder for reconstruction. sg is the stop-gradient operation, and β is a hyper-parameter to balance the commitment loss Oord et al. (2017). The quantized codebook index is determined by looking up the nearest codebook vector of input features $E(v)$ in terms of the Euclidean distance. The VQGAN Esser et al. (2021) is a variant of VQVAE, which adds a perceptual loss and an adversarial loss produced by patch-based discriminator. It can achieve high resolution while significantly reducing the sequence length. The complete objective for the compression model Q^* is:

$$Q^* = \arg\min_{G,C,E} \max_{D} \mathbb{E}_{x\sim p(v)}[\mathcal{L}_{VQ}(G,C,E) + \lambda\mathcal{L}_{GAN}(\{G,C,E\},D)], \tag{2}$$

where $\mathcal{L}_{GAN}$ is to learn the differences between real and reconstructed images:

$$\mathcal{L}_{GAN}(\{G,C,E\},D) = [\log D(v) + \log(1-D(\hat{v}))]. \tag{3}$$

Auto-regressive Transformer Based on the first stage, the images can be highly compressed by the codebook-indices of their embeddings. In this state, the image encoder E is fixed. Therefore, the $\mathbf{V}$, $\mathbf{T}$, $\mathbf{M}$, and $\mathbf{A}$ can be represented by the embedding $\mathbb{S}$ of the sequence of tokens. We adopt the axial positional embedding $\mathbb{P}$ to process the codebook-indices generating by the image reconstruction module $\mathbb{R}$, which is practically effective for multi-dimensional data. In our implementation, the sequence T_{seq} of the transformer is sequentially formed by $\mathbf{T}$, $\mathbf{V}$, $\mathbf{M}$, and $\mathbf{A}$, which is defined as follows:

$$T_{seq} = \text{Concat}(\mathbb{S}(\mathbb{O}(T)), \mathbb{P}(\mathbb{R}(V)), \mathbb{P}(\mathbb{R}(M)), \mathbb{S}(\mathbb{O}(A))), \tag{4}$$

which focuses to generate the re-created result and textual feedback. $\mathbb{O}$ represents the tokenize operation. The transformer is designed as a decoder-only model, which is same as Child et al. (2019). In our architecture, text tokens have the ability to attend to each image token in any of the self-attention layers. The model employs two types of self-attention masks. The attention masks used for text-to-text attention follow the conventional causal mask. On the other hand, for image-to-image attention, the model applies either a row, column, or convolutional attention mask in different self-attention layer, as explained in Child et al. (2019); Ramesh et al. (2021a). During training, each token is asked to predict the distribution of the next token, which formulates as an autoregressive next-index prediction. Therefore, it is equivalent to maximize the log-likelihood of the data representations.

$$\mathcal{L}_{Transformer} = \mathbb{E}_{x\sim p(x)}[-\log p(T_{seq})], \tag{5}$$

where p is the full representation of the likelihood of the possible next indices. Note that for the "cannot" and "forbidden" pairs, as there is no re-created ground truth, the loss of the its prediction will not be back-propagated. We have tried to predict a black image or the original visual input for these two cases, but both of them perform much worse than simply ignoring their loss. In the testing procedure, we only need to input the $\mathbf{T}$ and $\mathbf{V}$ for pixel-wise iterative generation until the required length is achieved.

4 Experiment

In this section, we introduce the experimental details, evaluation metrics, and analyse on the quantitative and qualitative results.

Table 4: Qualitative results of CLEVR-ATVC dataset.

Visual (V)	Text (T)	Re-created (M)	Answer (A)	**FM-Score**
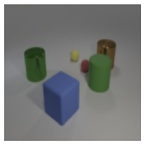	Please exchange the positions of the large brown metal cylinder and the large blue rubber cube.		No problem.	**1.0**
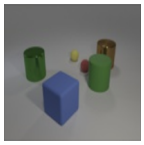	Please put the large brown metal cylinder on top of the large blue rubber cube.	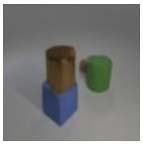	No problem.	**0.75**
	Please put the small gray rubber cylinder on top of the large yellow metal cube.	/	This action cannot be done. Because there is no large yellow metal cube.	**1.0**
	Please put the small gray metal sphere under the small purple rubber cylinder.	/	This action is forbidden. Because you cannot put the sphere under an object, and there is no small gray metal sphere and no small purple rubber cylinder.	**1.0**

Table 5: Image re-creation evaluation on the CLEVR-ATVC dataset.

PSNR	SSIM	FSIM	Human Rank (%)				
			A	B	C	Score	FM-Score
55.0	0.9944	0.669	25.9	16.2	58.0	39.0	52.6

4.1 Experimental Details

All experiments are all conducted with Pytorch 1.8.1. The model parameters are updated through Adam Diederik P. Kingma (2014) with $\beta_1 = 0.9$, $\beta_2 = 0.999$. We first trains the image reconstruction module for 200 epochs with an initial learning rate of 0.001 and a decay rate of 0.99 per epoch. This stage takes about half a day to train for 200 epochs. The number of attention heads, the attention key and value dimensions, the number of layers, and the dimensions of the models are set to 8, 64, 4, and 512, respectively. The text tokenizer operates on a lower-cased byte pair encoding (BPE) representation of the text with a 49,408 vocab size Sennrich R & A (2015). The text sequence is bracketed with [SOS] and [EOS] tokens. The maximum length of the text sequence is set to 64, and the output length of the image codebook is 1024, which results in a total 2112 sequence lengths for the transformer model. The second stage is distributively trained over 200 epochs with a fixed learning rate of 0.0003. Unless specified, all the parameters of the architecture for the following experiments will remain the same. The model is trained for approximate 900 GPU days on CLEVR-ATVC dataset and 350 GPU days on Fruit-ATVC dataset.

4.2 Evaluation Metrics

We evaluate the proposed method using the following two types of metrics.

Table 6: Texual feedback evaluation on the CLEVR-ATVC dataset. Type Acc. represents that the answer can correctly recognize the query that cannot be done or forbidden. Exp Acc. represents the explanation is correct in both answer type and the reasons.

Can		Cannot			Forbidden			Score (%)
Num	Acc.	Num	Type Acc.	Exp Acc.	Num	Type Acc.	Exp Acc.	
1662	71.6%	1997	49.4%	46.5%	1341	99.7%	58.2%	66.2

Image Quality Metric. The first two are the Peak signal-to-noise ratio (PSNR) and the structural similarity index measure (SSIM), which are commonly used to measure the similarity and quantify reconstruction quality of images. We also adopt the FSIM metric Zhang et al. (2011), which could be more suitable for the human visual system (HVS) using phase congruency (PC) and gradient magnitude (GM).

Human Evaluation. Following the previous methods Lee et al. (2020); Ding et al. (2021); Dong et al. (2017); Zhang et al. (2017; 2018; 2020); Kayser et al. (2021), we also adopt Human Rank (HR) to precisely reveal the performance. HR can be used to evaluate whether the synthesized image conforms to subjective effects (authenticity, matching degree with text, etc.). We set three different classes for the HR: a) if the action is perfectly done, the result would be ranked "A", representing score 1; b) if the action is correct, but other parts are affected, *e.g.*, mistakenly change the color or erasing other irrelevant objects, the result would be ranked "B", representing score 0.5; c) if the action is incorrect, the result is "C", representing score 0. Therefore, the final HR score is between 0 and 1, and the Full-Match score (FM-Score) represents that both the re-creation and the answer are correct. The higher scores of all metrics, the better performance is represented. The "accountable" part is totally automatic, for which we use the full string matching to measure the accuracy between ground truth answers and the final predictions. We also take into account that the textual feedback in the explanation part will change, such as that both explanations "There is no object1 and object2" and "There is no object2 and object1" are correct. We also designed tools to help with human evaluation, and we provide its interface and evaluation criteria in the appendix. In addition, we assign 100 sets of results to 5 works for scoring, we empirically find that our task usually has an explicit answer which is not easily affected by human subjective opinions.

4.3 Results and Analyses

In this section, we evaluate the proposed method on the CLEVR-ATVC and Fruit-ATVC datasets, whose results include the image re-creation, textual feedback, qualitative visualizations and the model behavior when facing uncertainty.

4.3.1 Results on CLEVR-ATVC

For the CLEVR-ATVC dataset, the re-created results are shown in Table 5. We can see that the machine achieves FM-Score 52.6% (re-creation and textual feedback are completely correct), which also shows the difficulty of the task. The high SSIM 0.9944 represents the model can obtain high image reconstruction quality. Based on our observation, we find that the "exchange color" queries are mostly correct, while "exchange positions" queries are somewhat limited by the image reconstruction.

The quantitative results of textual feedback are shown in Table 6. We can see that there are 1662 pairs for the results on "can" queries; among them, 71.6% pairs are answered correctly. For the queries about "cannot", 49.4% pairs can be accurately recognized that the query is not doable, and 46.5% pairs can not only answer the type but correctly answer the reasons. For the queries about "forbidden", 99.7% can be correctly recognized, but only 58.2% can correctly explain the reasons. The score is the weighted average of the above results. As there are numerous possible answers, a random guessing result is less than 1%, and thus it should be safe to conclude that the proposed method has shown impressive results.

Example qualitative results are shown in Table 4. We can conclude that the model can cay "No" to instructions and give accurate language-based explanations. In addition, it is worth mentioning that the model

Table 7: Qualitative results of the Fruit-ATVC dataset.

Visual (V)	Text (T)	Re-created (M)	Answer (A)	**FM-Score**
	Please remove the plate.	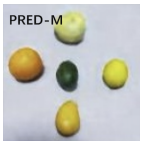	No problem.	**1.0**
	Please put the lemon in the bowl.		No problem.	**0.75**
	Please exchange the position of the banana and the coconut.	/	This action cannot be done. Because there is no coconut.	**1.0**
	Please remove the bottle.	/	This action cannot be done. Because there is no kiwi and no bottle.	**0.75**

Table 8: Image re-creation evaluation on the Fruit-ATVC dataset.

PSNR	SSIM	FSIM	Human Rank (%)				
			A	B	C	Score	FM-Score
44.1	0.9272	0.420	12.8	29.4	57.9	27.5	46.1

also implicitly learns the depth of the image and size of the objects, and thus it knows whether the object is occluded and how much it is occluded when you manipulate some objects.

4.3.2 Results on Fruit-ATVC

For the Fruit-ATVC dataset, the re-created results are shown in Table 8. The final score for re-creation is 46.1%, which results can produce both correct re-creation as well as the textual feedback. These results also demonstrate the the difficulty of the task, especially in real scenarios.

The quantitative results of answers are shown in Table 9. We can see that 78.3% of "can" queries can be answered correctly, and 25.0% queries about "cannot" can be correctly explained. In the "exchange position" queries, we find that although it can perform correct re-creation, the reconstruction for other objects is challenging. For the "put in" queries, the errors usually occur by creating a new target fruit without erasing it in the image. The re-creation results of the "remove" are the best among three actions. All the results suggest the challenges of this dataset of real scenes. Example qualitative results are shown in Table 7.

4.3.3 Uncertainty of Image Re-creation

In this section, we would like to explore whether the model can handle the uncertainty appeared in the query. The results show that our method deals with emerging uncertainties well. As shown in Table 12, all the image re-creation results get ranking A, except for the result of the last row. The score B is due to an object being erased during image reconstruction, not due to uncertainty. For example, as shown in the

Table 9: Textual feedback evaluation on the Fruit-ATVC dataset.

Can		Cannot			Score
Num	Acc.	Num	Type Acc.	Exp Acc.	
950	78.3%	922	77.2%	25.0%	64.7%

Table 10: Evaluation results on the CLEVR-ATVC sub-dataset.

Methods	Image	PSNR	SSIM	FSIM	Human Rank (%)			
					A	B	C	Score
Ours w/ VQVAE	128×128	**56.6**	**0.9963**	**0.693**	**66.4**	14.8	18.8	**73.8**
Ours w/ VQGAN	256×256	53.9	0.9947	0.604	52.7	**27.4**	**19.9**	66.4

fourth row of Table 12, our model only exchanges the position of one "small yellow rubber cube", which is consistent with the settings in our constructed dataset. The "exchange position" only needs to process one of the objects, but "exchange color" needs to exchange the colors of all satisfied objects. Existing models are able to make different decisions for the above different situations, so our method shows a good behavior.

4.4 Single Action without Answer

In this section, we firstly evaluate the image auto-encoder method VQVAE Oord et al. (2017) with short query and the imperfect query on the CLEVR-ATVC sub-dataset. We only select one "put on top" action without textual feedback for verification and evaluation.

4.4.1 Short or Imperfect Query for Re-creation

We would like to verify the results on the short query of the CLEVR-ATVC sub-dataset. The short query means that we remove redundant text in the query, such as "please", "put", and "the" are removed, while the latter randomly removes keywords (such as "color", "size" or "shape"). The quantitative results shown in Table 11 show that the intact queries (long text) perform slightly better than the removed version (short text).

The visualization results are shown in Figure 4, with the observations on the imperfect queries: a) If the "blue" is removed from query, the generated cylinder seems to be shorter; b) If the query contains a nonexistent "blue" adjective for the cube, the model creates one; c) If both the nonexistent "blue" cube and "cyan" cylinder coexist in the same query, the model seems to mistakenly recognize the cyan cube, and we can find the small gray cylinder is also erased, which is incorrect; d) If we simply remove the "cube", the model just dyes a litter red on top of the cylinder; e) If we remove the "please put", the result just remains the original figure; f) If we add the unseen word, *e.g.*, "amazing", in the query, the manipulation result can still be achieved. We further test a lot of images, which show that the unlearned "create" and "dye" abilities commonly appear but not always. The above results also suggest that if we don't add restriction rules to the dataset, then the model will satisfy human instructions by creating new objects, and this uncontrollability is not the desired outcome. Therefore, it is necessary to regulate the behavior of the model by adding pre-set rules as supervision signals.

4.4.2 VQVAE vs. VQGAN

In this section, we evaluate the image auto-encoder methods, VQVAE Oord et al. (2017) and VQGAN Esser et al. (2021), on the CLEVR-ATVC sub-dataset. We only select one "put on top" action without textual feedback for evaluation. As shown in Table 11, although VQGAN-based image auto-encoder can output a large resolution and at 4 times faster of training than the VQVAE counterpart, the latter is 7.4% better. The results shown in Figure 5 and B4 show that VQGAN-based image encoder always changes the color of objects, erases objects and add irrelevant objects on the re-created images. These results also demonstrate

Table 11: Evaluation results on the CLEVR-ATVC sub-dataset.

Methods	Text	Image	PSNR	SSIM	FSIM	Human Rank (%)			
						A	B	C	Score
Ours w/ VQVAE	Short	128 × 128	56.3	0.9957	0.689	65.9	14.4	**19.7**	71.9
Ours w/ VQVAE	Long	128 × 128	**56.6**	**0.9963**	**0.693**	**66.4**	**14.8**	18.8	**73.8**

Table 12: Uncertainty evaluation on CLEVR-ATVC dataset.

Visual (V)	Text (T)	Re-created (M)	Answer (A)	**Ranking**
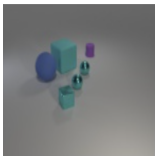	Please exchange the color of the large blue rubber sphere and the small purple rubber cylinder.		No problem.	**A**
	Please exchange the color of the large purple metal cube and the large red metal cylinder.		No problem.	**A**
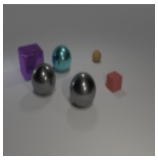	Please exchange the color of the large cyan metal sphere and the small red rubber cube.		No problem.	**A**
	Please exchange the position of the small yellow rubber cube and the small purple rubber cube.		No problem.	**A**
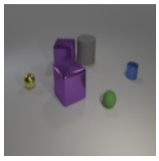	Please exchange the color of the large purple metal cube and the small blue metal cylinder.		No problem.	**A**
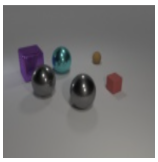	Please put the large purple metal cube under the large gray metal sphere.		No problem.	**B**

that VQGAN can produce high-quality images using fewer computational resources, but it appears to have lost its ability to discriminate on object properties in latent space.

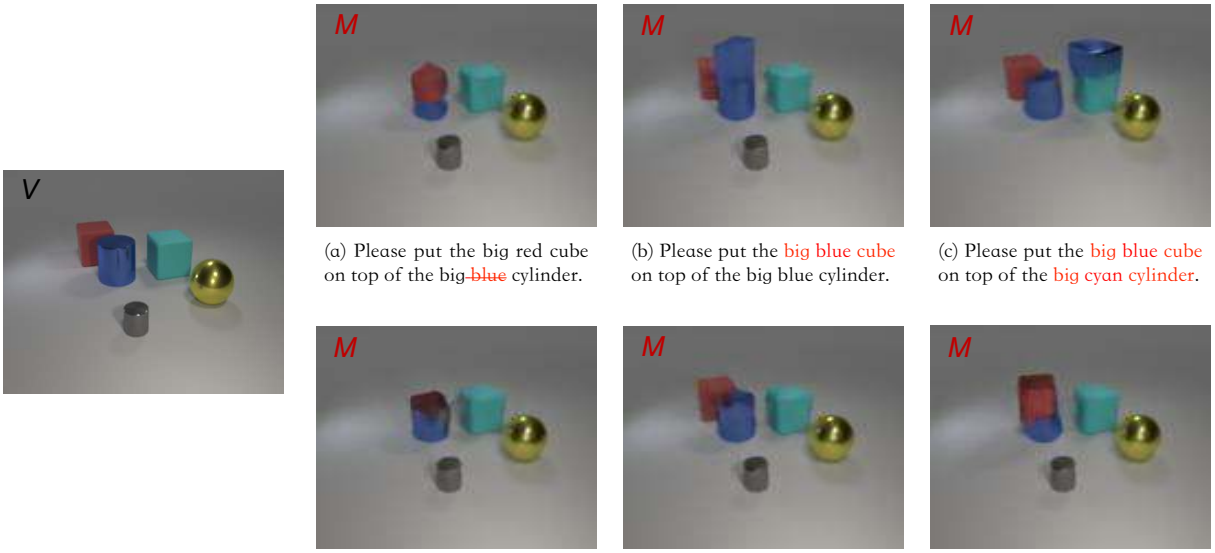

(a) Please put the big red cube on top of the big ~~blue~~ cylinder.

(b) Please put the big blue cube on top of the big blue cylinder.

(c) Please put the big blue cube on top of the big cyan cylinder.

(d) Please put the big red ~~cube~~ on top of the big blue cylinder.

(e) ~~Please put~~ the big red cube on top of the big blue cylinder.

(f) Please put the amazing big red cube on top of the amazing big blue cylinder.

Figure 4: Image re-creation results on the CLEVR-ATVC sub-dataset using imperfect query. The red text represents the short or imperfect query.

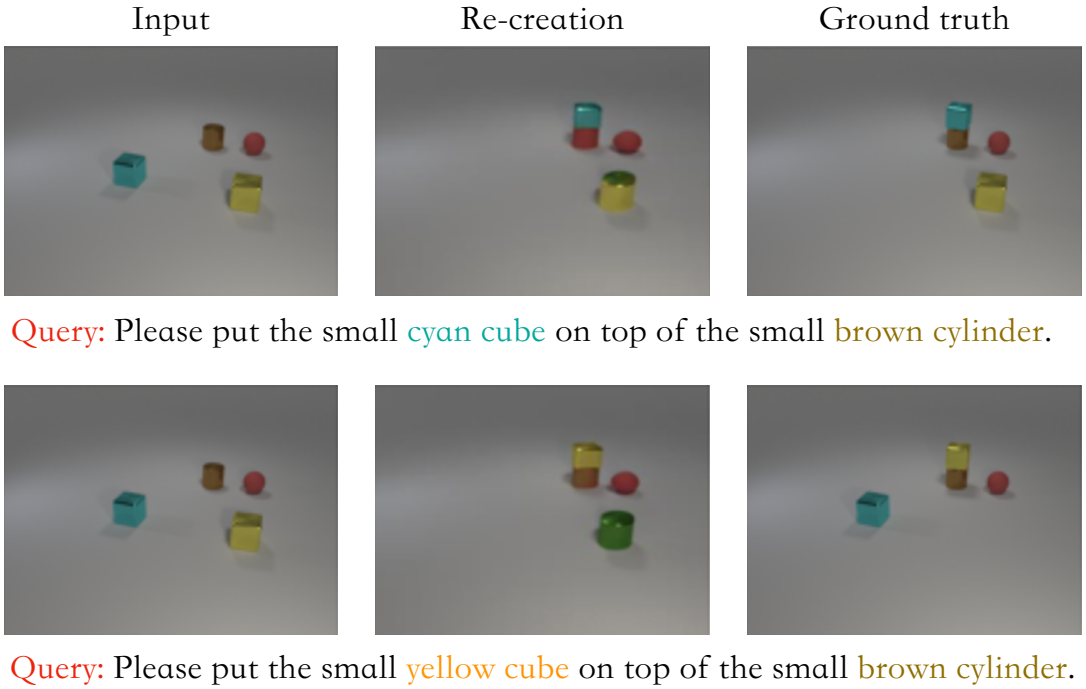

Figure 5: Analyse for the results of VQGAN-based image encoder. VQGAN frequently changes the colors of the objects, which downgrades the performance.

5 Related works

In this section, we first review some representative datasets and methods on vision-and-language tasks whose inputs and outputs are always unimodal. Next, we introduce the prior multimodal dialogue models. Finally,

we briefly summarize the recent controllable text-to-image generation methods and the main differences between them and our task.

5.1 Vision-and-Language Tasks

Recent years have witnessed the rapid development of vision-and-language tasks. Their development trend can be observed through the construction of the datasets, which can be roughly categorized into two groups: *Vision to Language*, *Language to Vision*. We briefly summarize these relevant datasets and methods.

Vision to Language. There are several sub-tasks for this category such as *Visual Description Generation* Ordonez et al. (2011), *Visual Storytelling* Lin et al. (2014), *Visual Dialog* Das et al. (2017); Kottur et al. (2019), *Visual Entailment* Vu et al. (2018); Liu et al. (2020), *Visual Reasoning* Johnson et al. (2017), *Visual Question Answering* Antol et al. (2015); Marino et al. (2019) and *Visual Referring Expression* Liu et al. (2019).

- Visual Description Generation, a.k.a., captioning, is the most well-known task, where many datasets in the past decade are constructed to address different scales, scenes, etc. For examples, image captioning datasets, SBU1M Ordonez et al. (2011), Flickr8k Hodosh et al. (2013), Flickr30k Young et al. (2014), MSCOCO Lin et al. (2014), Multi30k-CLID Elliott et al. (2016), Flickr30k-Entities Plummer et al. (2015), STAIR Captions Yoshikawa et al. (2017), Conceptual Captions Sharma et al. (2018), MSCOCO-Entities Cornia et al. (2019), Personality Captions Shuster et al. (2019) and video captioning datasets, MSVD Chen & Dolan (2011), MPII Cooking Rohrbach et al. (2012), YouCook Das et al. (2013), TACoS Regneri et al. (2013), TACoS-MultiLevel Rohrbach et al. (2014), M-VAD Torabi et al. (2015), MSR-VTT Xu et al. (2016), VTW Zeng et al. (2016), ANetCap Krishna et al. (2017), YouCook II Zhou et al. (2018), ANetEntities Zhou et al. (2019), COIN Tang et al. (2019), HowTo100M Miech et al. (2019), have played an important role in advancing visual captioning.

- Visual Storytelling usually requires the methods to generate a series of text to describe a set or a sequence of the visual inputs, as shown in several datasets: NYC-Storytelling Park & Kim (2015), Disneyland Storytelling Kim et al. (2015), SIND, and VIST Huang et al. (2016).

- Visual Dialog can be regarded as a natural conversation system based on the image or video. Examples can be found in the existing benchmarks such as VisDial Das et al. (2017), CLEVR-Dialog Kottur et al. (2019) and AVSD Alamri et al. (2018).

- Visual Entailment is introduced in V-SNLI Vu et al. (2018), SNLI-VE Xie et al. (2019), and VIOLIN Liu et al. (2020), which requires the method to learn to select the correct premise and hidden semantic information that can be inferred from the visual contents.

- Vision Reasoning is expected to provide the scene graphs between objects and then to answer questions based on the visual input and relationships. Many datasets such as CLEVR Johnson et al. (2017), NLVR Suhr et al. (2017), CLEVR-CoGenT Yang et al. (2018), NLVR2 Suhr et al. (2018), GQA Hudson & Manning (2019), VCR Zellers et al. (2019), and Visual COMET Park et al. (2020) have been constructed between 2017 and 2020, which demonstrate visual reasoning abilities can be effectively learned by the deep neural networks LeCun et al. (2015).

- Visual Question Answering is another representative vision-to-language task, in which the model is expected to generate text-based answer according to the question and the visual cues. The most influential dataset VQA v1.0 Antol et al. (2015) as well as MovieQA Tapaswi et al. (2016), TVQA Lei et al. (2018), OK-VQA Marino et al. (2019), KVQA Shah et al. (2019), and VQA v2.0. Antol et al. (2015) have greatly promoted the development.

- Visual Referring Expression is another task which requires the method to comprehend the referring expressions by showing evidence in the visual images, *i.e.*, using bounding boxes to locate the corresponding objects. There are several datasets targeting this task, such as RefCLEF Kazemzadeh et al. (2014), and CLEVR-Ref+4 Liu et al. (2019).

Language to Vision. This task aims at image generation based on the pure natural language. Currently, there are only a few datasets for this task such as Oxford-102 Reed et al. (2016), Caltech-UCSD Birds (CUB) Reed et al. (2016), Multi-Modal-CelebA-HQ Xia et al. (2021), Text2Human Jiang et al. (2022), Laion-400M Schuhmann et al. (2021), Laion-5B Schuhmann et al. (2022) and Text2Video Xu et al. (2016); Li et al. (2018); Hong et al. (2022); Ho et al. (2022); Khachatryan et al. (2023); **?**. These datasets are similar to the vision-to-language task above, and the text-image pairs contain text descriptions of the image content. The most representative task is text-based image generation, which has recently seen large progress in multimodal learning Brooks et al. (2023); Li et al. (2023b). Many previous works train GANs with text-conditioning on publicly available image captioning datasets Tao et al. (2020); Zhang et al. (2021). DALL·E Ramesh et al. (2021b) uses 250 million text-image pairs to successfully achieve promising results, which can even perform zero-shot visual reasoning by using some prompts. Another zero-shot model termed CLIP Radford et al. (2021) is used to rank and measure the similarity between image and text, as usually one text prompt can produce numerous plausible results. The recent DALL·E 2 Ramesh et al. (2022) uses a diffusion prior on CLIP text latents and cascaded diffusion models to generate high resolution 1024×1024 images. GLIDE Nichol et al. (2021) also applies guided diffusion to the problem of text-conditional image synthesis. Imagen Saharia et al. (2022) combines the power of transformer language models with high-fidelity diffusion models to deliver an unprecedented degree of photorealism in text-to-image synthesis.

In contrast to the aforementioned datasets that typically concentrate on one aspect, our proposed datasets introduce a novel requirement for models to generate both visual re-creations and textual feedback simultaneously. The visual manipulation aspect necessitates not only performing the required actions accurately but also preserving a visually plausible background. Simultaneously, the feedback generated by the models needs to be aware of the possibilities of feasible actions, actions that cannot be performed, and actions that are explicitly prohibited. This requirement ensures that the datasets possess both value and challenge.

5.2 Multimodal Dialogue Models

The task of vision-to-language involves using visual samples as input and generating text as output, as seen in tasks like Visual Dialog. Conversely, language-to-vision tasks operate in the opposite direction. In multimodal dialogue methods, the model must reason about multimodal or unimodal inputs and produce multimodal or unimodal outputs. These methods can be categorized into the following two types:

- *Multimodal Input and Unimodal Output (MIUO)*: This conversational task is similar to visual dialog, where the input typically consists of visual data and text-based prompts (i.e., multimodal input). The visual language model performs visual reasoning on the image and provides an answer (i.e., unimodal output) Alayrac et al. (2022); Brooks et al. (2023); Gong et al. (2023); Bo Li (2023); Li et al. (2023a); OpenAI (2023b); Su et al. (2023); Yang et al. (2023b); Zhao et al. (2023); Zhu et al. (2023); Liu et al. (2023); Mu et al. (2023); Wang et al. (2023); Zhang et al. (2023). GPT-4 OpenAI (2023b) and MultiModal-GPT Gong et al. (2023) can handle prompts consisting of interleaved visual inputs and text-based queries, generating text outputs. VideoChat Li et al. (2023a) introduces a video-centric multimodal dialogue dataset, enabling trained models to understand and generate detailed conversations about videos.

- *Multimodal Input and Multimodal Output (MIMO)*: This task requires the model to perform multimodal reasoning and generation simultaneously Koh et al. (2023); Jing Yu Koh (2023); Chenfei Wu & Duan (2023); Yang et al. (2023a). Visual ChatGPT Chenfei Wu & Duan (2023) is a pioneering work that combines ChatGPT and a series of pre-trained visual foundation models, allowing them to accept and produce text and images during textual-visual conversations. GILL Koh et al. (2023) proposes a mapping network that efficiently maps the output embedding space of a frozen text-only language model to that of a frozen generation model (e.g., Stable Diffusion Rombach et al. (2022)). This mapping only requires fine-tuning a small number of parameters on image-caption pairs for tasks such as image retrieval, novel image generation, and multimodal dialogue. FROMAGe Jing Yu Koh (2023) also involves image-text inputs and outputs for multimodal dialogue, with a few linear layers fine-tuned while keeping the pre-trained language model frozen. GPT4Tools Yang et al.

(2023a) introduces an instruction dataset and extends Visual ChatGPT Chenfei Wu & Duan (2023) to the image understanding task.

5.3 Controllable Text-to-image Generation

The above text-based image generation methods primarily focus on generating high-quality images based on given text descriptions, without providing the user with the ability to manipulate specific visual attributes using natural language instructions Anderson et al. (2018); Nguyen et al. (2019); Thomason et al. (2020); Cheng et al. (2014); Scalise et al. (2018); Stepputtis et al. (2020); Nam et al. (2018); Yüksel et al. (2021); Shen et al. (2020); Li et al. (2020); Richardson et al. (2020); Esser et al. (2021). However, some recent works have explored techniques to control the synthesis process by representing scenes as compositional generative neural feature fields, enabling the disentanglement of objects from the background, as well as individual objects' shapes and appearances Li et al. (2019); Bodla et al. (2018); Nam et al. (2018); Chen et al. (2021); Shuster et al. (2019). For instance, ControlGAN Li et al. (2019) can synthesize high-quality images while allowing control over specific parts of the image generation based on natural language descriptions. FusedGAN Bodla et al. (2018) achieves enhanced controllability in sampling by disentangling different factors in the latent space. Text2Human Jiang et al. (2022) can synthesize human images by specifying clothing shapes and textures solely through natural language descriptions.

However, the aforementioned approaches focus on controlling the image generation process through composition or disentanglement techniques. In this paper, our objective is to control the outcomes of re-created images, where the system learns to respond with a "no" to commands that are either prohibited or cannot be executed.

6 Conclusion

In this paper, we raise an important yet underexplored concern regarding the accountability of multimodal generative models. To tackle this issue, we introduce two novel datasets, namely CLEVR-ATVC and Fruit-ATVC, designed for a unique task called Accountable Text-based Visual Re-creation. The objective of this task is to train Visual Language Models (VLMs) to reject human instructions. Our datasets consist of both visual and textual inputs and outputs, requiring the model to perform visual re-creation while ensuring image quality when the answer is "yes". In cases where the model cannot complete the action or the action is prohibited, it is required to provide an explanation. We provide baseline models, experimental settings, evaluation metrics, and a comprehensive analysis, presenting some promising results. These high-quality datasets can also be utilized in similar tasks, and we hope that our work inspires further research on the accountability problem, encompassing model design, label annotation, and the creation of larger datasets. We firmly believe that addressing the issue of accountability is crucial for advancing the development and deployment of multimodal generative models.

References

Huda Alamri, Chiori Hori, Tim K Marks, Dhruv Batra, and Devi Parikh. Audio visual scene-aware dialog (avsd) track for natural language generation in dstc7. In *DSTC7 at AAAI2019 Workshop*, volume 2, 2018.

Jean-Baptiste Alayrac, Jeff Donahue, Pauline Luc, Antoine Miech, Iain Barr, Yana Hasson, Karel Lenc, Arthur Mensch, Katherine Millican, Malcolm Reynolds, et al. Flamingo: a visual language model for few-shot learning. *Advances in Neural Information Processing Systems*, 35:23716–23736, 2022.

Peter Anderson, Qi Wu, Damien Teney, Jake Bruce, Mark Johnson, Niko Sünderhauf, Ian Reid, Stephen Gould, and Anton Van Den Hengel. Vision-and-language navigation: Interpreting visually-grounded navigation instructions in real environments. In *Proceedings of the IEEE Conference on Computer Vision and Pattern Recognition*, pp. 3674–3683, 2018.

Stanislaw Antol, Aishwarya Agrawal, Jiasen Lu, Margaret Mitchell, Dhruv Batra, C Lawrence Zitnick, and Devi Parikh. Vqa: Visual question answering. In *Proceedings of the IEEE international conference on computer vision*, pp. 2425–2433, 2015.

Liangyu Chen Jinghao Wang Fanyi Pu Jingkang Yang Chunyuan Li Ziwei Liu Bo Li, Yuanhan Zhang. Mimic-it: Multi-modal in-context instruction tuning. *arXiv preprint arXiv:2306.05425*, 2023.

Navaneeth Bodla, Gang Hua, and Rama Chellappa. Semi-supervised fusedgan for conditional image generation. In *Proceedings of the European conference on computer vision (ECCV)*, pp. 669–683, 2018.

Tim Brooks, Aleksander Holynski, and Alexei A Efros. Instructpix2pix: Learning to follow image editing instructions. In *Proceedings of the IEEE/CVF Conference on Computer Vision and Pattern Recognition*, pp. 18392–18402, 2023.

David Chen and William B Dolan. Collecting highly parallel data for paraphrase evaluation. In *Proceedings of the 49th Annual Meeting of the Association for Computational Linguistics: Human Language Technologies*, pp. 190–200, 2011.

Tianyi Chen, Yi Liu, Yunfei Zhang, Si Wu, Yong Xu, Feng Liangbing, and Hau San Wong. Semi-supervised single-stage controllable gans for conditional fine-grained image generation. In *Proceedings of the IEEE/CVF International Conference on Computer Vision*, pp. 9264–9273, 2021.

Weizhen Qi Xiaodong Wang Zecheng Tang Chenfei Wu, Shengming Yin and Nan Duan. Visual chatgpt: Talking, drawing and editing with visual foundation models. *arXiv preprint arXiv:2303.04671*, 2023.

Yu Cheng, Yunyi Jia, Rui Fang, Lanbo She, Ning Xi, and Joyce Chai. Modelling and analysis of natural language controlled robotic systems. *IFAC Proceedings Volumes*, 47(3):11767–11772, 2014.

Rewon Child, Scott Gray, Alec Radford, and Ilya Sutskever. Generating long sequences with sparse transformers. *arXiv preprint arXiv:1904.10509*, 2019.

Marcella Cornia, Lorenzo Baraldi, and Rita Cucchiara. Show, control and tell: A framework for generating controllable and grounded captions. In *Proceedings of the IEEE/CVF Conference on Computer Vision and Pattern Recognition*, pp. 8307–8316, 2019.

Abhishek Das, Satwik Kottur, Khushi Gupta, Avi Singh, Deshraj Yadav, José MF Moura, Devi Parikh, and Dhruv Batra. Visual dialog. In *Proceedings of the IEEE Conference on Computer Vision and Pattern Recognition*, pp. 326–335, 2017.

Pradipto Das, Chenliang Xu, Richard F Doell, and Jason J Corso. A thousand frames in just a few words: Lingual description of videos through latent topics and sparse object stitching. In *Proceedings of the IEEE conference on computer vision and pattern recognition*, pp. 2634–2641, 2013.

Jimmy Ba Diederik P. Kingma. Adam: A method for stochastic optimization. *arXiv preprint arXiv:1412.6980*, 2014.

Ming Ding, Zhuoyi Yang, Wenyi Hong, Wendi Zheng, Chang Zhou, Da Yin, Junyang Lin, Xu Zou, Zhou Shao, Hongxia Yang, et al. Cogview: Mastering text-to-image generation via transformers. *arXiv preprint arXiv:2105.13290*, 2021.

Hao Dong, Simiao Yu, Chao Wu, and Yike Guo. Semantic image synthesis via adversarial learning. In *Proceedings of the IEEE International Conference on Computer Vision*, pp. 5706–5714, 2017.

Finale Doshi-Velez, Mason Kortz, Ryan Budish, Chris Bavitz, Sam Gershman, David O'Brien, Kate Scott, Stuart Schieber, James Waldo, David Weinberger, et al. Accountability of ai under the law: The role of explanation. *arXiv preprint arXiv:1711.01134*, 2017.

Desmond Elliott, Stella Frank, Khalil Sima'an, and Lucia Specia. Multi30k: Multilingual english-german image descriptions. *arXiv preprint arXiv:1605.00459*, 2016.

Patrick Esser, Robin Rombach, and Björn Ommer. Taming transformers for high-resolution image synthesis. *CVPR*, 2021.

Tao Gong, Chengqi Lyu, Shilong Zhang, Yudong Wang, Miao Zheng, Qian Zhao, Kuikun Liu, Wenwei Zhang, Ping Luo, and Kai Chen. Multimodal-gpt: A vision and language model for dialogue with humans. *arXiv preprint arXiv:2305.04790*, 2023.

Jonathan Ho, Tim Salimans, Alexey Gritsenko, William Chan, Mohammad Norouzi, and David J Fleet. Video diffusion models. *arXiv preprint arXiv:2204.03458*, 2022.

Micah Hodosh, Peter Young, and Julia Hockenmaier. Framing image description as a ranking task: Data, models and evaluation metrics. *Journal of Artificial Intelligence Research*, 47:853–899, 2013.

Wenyi Hong, Ming Ding, Wendi Zheng, Xinghan Liu, and Jie Tang. Cogvideo: Large-scale pretraining for text-to-video generation via transformers. *arXiv preprint arXiv:2205.15868*, 2022.

Ting-Hao Huang, Francis Ferraro, Nasrin Mostafazadeh, Ishan Misra, Aishwarya Agrawal, Jacob Devlin, Ross Girshick, Xiaodong He, Pushmeet Kohli, Dhruv Batra, et al. Visual storytelling. In *Proceedings of the 2016 Conference of the North American Chapter of the Association for Computational Linguistics: Human Language Technologies*, pp. 1233–1239, 2016.

Drew A Hudson and Christopher D Manning. Gqa: a new dataset for compositional question answering over real-world images. *arXiv preprint arXiv:1902.09506*, 2(3):11, 2019.

Yuming Jiang, Shuai Yang, Haonan Qju, Wayne Wu, Chen Change Loy, and Ziwei Liu. Text2human: Text-driven controllable human image generation. *ACM Transactions on Graphics (TOG)*, 41(4):1–11, 2022.

Daniel Fried Jing Yu Koh, Ruslan Salakhutdinov. Grounding language models to images for multimodal inputs and outputs. *arXiv preprint arXiv:2301.13823*, 2023.

Justin Johnson, Bharath Hariharan, Laurens Van Der Maaten, Li Fei-Fei, C Lawrence Zitnick, and Ross Girshick. Clevr: A diagnostic dataset for compositional language and elementary visual reasoning. In *Proceedings of the IEEE Conference on Computer Vision and Pattern Recognition*, pp. 2901–2910, 2017.

Maxime Kayser, Oana-Maria Camburu, Leonard Salewski, Cornelius Emde, Virginie Do, Zeynep Akata, and Thomas Lukasiewicz. e-vil: A dataset and benchmark for natural language explanations in vision-language tasks. *arXiv preprint arXiv:2105.03761*, 2021.

Sahar Kazemzadeh, Vicente Ordonez, Mark Matten, and Tamara Berg. Referitgame: Referring to objects in photographs of natural scenes. In *Proceedings of the 2014 conference on empirical methods in natural language processing (EMNLP)*, pp. 787–798, 2014.

Levon Khachatryan, Andranik Movsisyan, Vahram Tadevosyan, Roberto Henschel, Zhangyang Wang, Shant Navasardyan, and Humphrey Shi. Text2video-zero: Text-to-image diffusion models are zero-shot video generators. *arXiv preprint arXiv:2303.13439*, 2023.

Gunhee Kim, Seungwhan Moon, and Leonid Sigal. Ranking and retrieval of image sequences from multiple paragraph queries. In *Proceedings of the IEEE Conference on Computer Vision and Pattern Recognition*, pp. 1993–2001, 2015.

Jing Yu Koh, Daniel Fried, and Ruslan Salakhutdinov. Generating images with multimodal language models. *arXiv preprint arXiv:2305.17216*, 2023.

Satwik Kottur, José MF Moura, Devi Parikh, Dhruv Batra, and Marcus Rohrbach. Clevr-dialog: A diagnostic dataset for multi-round reasoning in visual dialog. *arXiv preprint arXiv:1903.03166*, 2019.

Ranjay Krishna, Kenji Hata, Frederic Ren, Li Fei-Fei, and Juan Carlos Niebles. Dense-captioning events in videos. In *Proceedings of the IEEE international conference on computer vision*, pp. 706–715, 2017.

Yann LeCun, Yoshua Bengio, and Geoffrey Hinton. Deep learning. *nature*, 521(7553):436–444, 2015.

Cheng-Han Lee, Ziwei Liu, Lingyun Wu, and Ping Luo. Maskgan: Towards diverse and interactive facial image manipulation. In *Proceedings of the IEEE/CVF Conference on Computer Vision and Pattern Recognition*, pp. 5549–5558, 2020.

Jie Lei, Licheng Yu, Mohit Bansal, and Tamara L Berg. Tvqa: Localized, compositional video question answering. *arXiv preprint arXiv:1809.01696*, 2018.

Bowen Li, Xiaojuan Qi, Thomas Lukasiewicz, and Philip Torr. Controllable text-to-image generation. *Advances in Neural Information Processing Systems*, 32, 2019.

Bowen Li, Xiaojuan Qi, Thomas Lukasiewicz, and Philip HS Torr. Manigan: Text-guided image manipulation. In *Proceedings of the IEEE/CVF Conference on Computer Vision and Pattern Recognition*, pp. 7880–7889, 2020.

KunChang Li, Yinan He, Yi Wang, Yizhuo Li, Wenhai Wang, Ping Luo, Yali Wang, Limin Wang, and Yu Qiao. Videochat: Chat-centric video understanding. *arXiv preprint arXiv:2305.06355*, 2023a.

Yitong Li, Martin Min, Dinghan Shen, David Carlson, and Lawrence Carin. Video generation from text. In *Proceedings of the AAAI Conference on Artificial Intelligence*, volume 32, 2018.

Yuheng Li, Haotian Liu, Qingyang Wu, Fangzhou Mu, Jianwei Yang, Jianfeng Gao, Chunyuan Li, and Yong Jae Lee. Gligen: Open-set grounded text-to-image generation. *arXiv preprint arXiv:2301.07093*, 2023b.

Tsung-Yi Lin, Michael Maire, Serge Belongie, James Hays, Pietro Perona, Deva Ramanan, Piotr Dollár, and C Lawrence Zitnick. Microsoft coco: Common objects in context. In *European conference on computer vision*, pp. 740–755. Springer, 2014.

Haotian Liu, Chunyuan Li, Qingyang Wu, and Yong Jae Lee. Visual instruction tuning. *arXiv preprint arXiv:2304.08485*, 2023.

Jingzhou Liu, Wenhu Chen, Yu Cheng, Zhe Gan, Licheng Yu, Yiming Yang, and Jingjing Liu. Violin: A large-scale dataset for video-and-language inference. In *Proceedings of the IEEE/CVF Conference on Computer Vision and Pattern Recognition*, pp. 10900–10910, 2020.

Runtao Liu, Chenxi Liu, Yutong Bai, and Alan L Yuille. Clevr-ref+: Diagnosing visual reasoning with referring expressions. In *Proceedings of the IEEE/CVF Conference on Computer Vision and Pattern Recognition*, pp. 4185–4194, 2019.

Michele Loi and Matthias Spielkamp. Towards accountability in the use of artificial intelligence for public administrations. In *Proceedings of the 2021 AAAI/ACM Conference on AI, Ethics, and Society*, pp. 757–766, 2021.

Kenneth Marino, Mohammad Rastegari, Ali Farhadi, and Roozbeh Mottaghi. Ok-vqa: A visual question answering benchmark requiring external knowledge. In *Proceedings of the IEEE/CVF Conference on Computer Vision and Pattern Recognition*, pp. 3195–3204, 2019.

Antoine Miech, Dimitri Zhukov, Jean-Baptiste Alayrac, Makarand Tapaswi, Ivan Laptev, and Josef Sivic. Howto100m: Learning a text-video embedding by watching hundred million narrated video clips. In *Proceedings of the IEEE/CVF International Conference on Computer Vision*, pp. 2630–2640, 2019.

Yao Mu, Qinglong Zhang, Mengkang Hu, Wenhai Wang, Mingyu Ding, Jun Jin, Bin Wang, Jifeng Dai, Yu Qiao, and Ping Luo. Embodiedgpt: Vision-language pre-training via embodied chain of thought. *arXiv preprint arXiv:2305.15021*, 2023.

Seonghyeon Nam, Yunji Kim, and Seon Joo Kim. Text-adaptive generative adversarial networks: manipulating images with natural language. *arXiv preprint arXiv:1810.11919*, 2018.

Khanh Nguyen, Debadeepta Dey, Chris Brockett, and Bill Dolan. Vision-based navigation with language-based assistance via imitation learning with indirect intervention. In *Proceedings of the IEEE/CVF Conference on Computer Vision and Pattern Recognition*, pp. 12527–12537, 2019.

Alex Nichol, Prafulla Dhariwal, Aditya Ramesh, Pranav Shyam, Pamela Mishkin, Bob McGrew, Ilya Sutskever, and Mark Chen. Glide: Towards photorealistic image generation and editing with text-guided diffusion models. *arXiv preprint arXiv:2112.10741*, 2021.

Michael Niemeyer and Andreas Geiger. Giraffe: Representing scenes as compositional generative neural feature fields. In *Proceedings of the IEEE/CVF Conference on Computer Vision and Pattern Recognition*, pp. 11453–11464, 2021.

Aaron van den Oord, Oriol Vinyals, and Koray Kavukcuoglu. Neural discrete representation learning. *arXiv preprint arXiv:1711.00937*, 2017.

OpenAI. Chatgpt. *https://openai.com/blog/chatgpt/*, 2023a.

OpenAI. Gpt-4 technical report. *arXiv preprint arXiv:2303.08774*, 2023b.

Vicente Ordonez, Girish Kulkarni, and Tamara Berg. Im2text: Describing images using 1 million captioned photographs. *Advances in neural information processing systems*, 24:1143–1151, 2011.

Cesc C Park and Gunhee Kim. Expressing an image stream with a sequence of natural sentences. *Advances in neural information processing systems*, 28:73–81, 2015.

Jae Sung Park, Chandra Bhagavatula, Roozbeh Mottaghi, Ali Farhadi, and Yejin Choi. Visualcomet: Reasoning about the dynamic context of a still image. In *European Conference on Computer Vision*, pp. 508–524. Springer, 2020.

Or Patashnik, Zongze Wu, Eli Shechtman, Daniel Cohen-Or, and Dani Lischinski. Styleclip: Text-driven manipulation of stylegan imagery. *arXiv preprint arXiv:2103.17249*, 2021.

Bryan A Plummer, Liwei Wang, Chris M Cervantes, Juan C Caicedo, Julia Hockenmaier, and Svetlana Lazebnik. Flickr30k entities: Collecting region-to-phrase correspondences for richer image-to-sentence models. In *Proceedings of the IEEE international conference on computer vision*, pp. 2641–2649, 2015.

Alec Radford, Jong Wook Kim, Chris Hallacy, Aditya Ramesh, Gabriel Goh, Sandhini Agarwal, Girish Sastry, Amanda Askell, Pamela Mishkin, Jack Clark, et al. Learning transferable visual models from natural language supervision. *arXiv preprint arXiv:2103.00020*, 2021.

Aditya Ramesh, Mikhail Pavlov, Gabriel Goh, Scott Gray, Chelsea Voss, Alec Radford, Mark Chen, and Ilya Sutskever. Zero-shot text-to-image generation. In *International Conference on Machine Learning*, pp. 8821–8831. PMLR, 2021a.

Aditya Ramesh, Mikhail Pavlov, Gabriel Goh, Scott Gray, Chelsea Voss, Alec Radford, Mark Chen, and Ilya Sutskever. Zero-shot text-to-image generation. *arXiv preprint arXiv:2102.12092*, 2021b.

Aditya Ramesh, Prafulla Dhariwal, Alex Nichol, Casey Chu, and Mark Chen. Hierarchical text-conditional image generation with clip latents. *arXiv preprint arXiv:2204.06125*, 2022.

Scott Reed, Zeynep Akata, Xinchen Yan, Lajanugen Logeswaran, Bernt Schiele, and Honglak Lee. Generative adversarial text to image synthesis. In *International Conference on Machine Learning*, pp. 1060–1069. PMLR, 2016.

Michaela Regneri, Marcus Rohrbach, Dominikus Wetzel, Stefan Thater, Bernt Schiele, and Manfred Pinkal. Grounding action descriptions in videos. *Transactions of the Association for Computational Linguistics*, 1:25–36, 2013.

Elad Richardson, Yuval Alaluf, Or Patashnik, Yotam Nitzan, Yaniv Azar, Stav Shapiro, and Daniel Cohen-Or. Encoding in style: a stylegan encoder for image-to-image translation. *arXiv preprint arXiv:2008.00951*, 2020.

Anna Rohrbach, Marcus Rohrbach, Wei Qiu, Annemarie Friedrich, Manfred Pinkal, and Bernt Schiele. Coherent multi-sentence video description with variable level of detail. In *German conference on pattern recognition*, pp. 184–195. Springer, 2014.

Marcus Rohrbach, Sikandar Amin, Mykhaylo Andriluka, and Bernt Schiele. A database for fine grained activity detection of cooking activities. In *2012 IEEE Conference on Computer Vision and Pattern Recognition*, pp. 1194–1201. IEEE, 2012.

Robin Rombach, Andreas Blattmann, Dominik Lorenz, Patrick Esser, and Björn Ommer. High-resolution image synthesis with latent diffusion models. In *Proceedings of the IEEE/CVF Conference on Computer Vision and Pattern Recognition*, pp. 10684–10695, 2022.

Chitwan Saharia, William Chan, Saurabh Saxena, Lala Li, Jay Whang, Emily Denton, Seyed Kamyar Seyed Ghasemipour, Burcu Karagol Ayan, S Sara Mahdavi, Rapha Gontijo Lopes, et al. Photorealistic text-to-image diffusion models with deep language understanding. *arXiv preprint arXiv:2205.11487*, 2022.

Rosario Scalise, Shen Li, Henny Admoni, Stephanie Rosenthal, and Siddhartha S Srinivasa. Natural language instructions for human–robot collaborative manipulation. *The International Journal of Robotics Research*, 37(6):558–565, 2018.

Christoph Schuhmann, Richard Vencu, Romain Beaumont, Robert Kaczmarczyk, Clayton Mullis, Aarush Katta, Theo Coombes, Jenia Jitsev, and Aran Komatsuzaki. Laion-400m: Open dataset of clip-filtered 400 million image-text pairs. *arXiv preprint arXiv:2111.02114*, 2021.

Christoph Schuhmann, Romain Beaumont, Richard Vencu, Cade Gordon, Ross Wightman, Mehdi Cherti, Theo Coombes, Aarush Katta, Clayton Mullis, Mitchell Wortsman, et al. Laion-5b: An open large-scale dataset for training next generation image-text models. *arXiv preprint arXiv:2210.08402*, 2022.

Haddow B Sennrich R and Birch A. Neural machine translation of rare words with subword units. *arXiv preprint arXiv:1508.07909v5*, 2015.

Sanket Shah, Anand Mishra, Naganand Yadati, and Partha Pratim Talukdar. Kvqa: Knowledge-aware visual question answering. In *Proceedings of the AAAI Conference on Artificial Intelligence*, volume 33, pp. 8876–8884, 2019.

Piyush Sharma, Nan Ding, Sebastian Goodman, and Radu Soricut. Conceptual captions: A cleaned, hypernymed, image alt-text dataset for automatic image captioning. In *Proceedings of the 56th Annual Meeting of the Association for Computational Linguistics (Volume 1: Long Papers)*, pp. 2556–2565, 2018.

Yujun Shen, Jinjin Gu, Xiaoou Tang, and Bolei Zhou. Interpreting the latent space of gans for semantic face editing. In *Proceedings of the IEEE/CVF Conference on Computer Vision and Pattern Recognition*, pp. 9243–9252, 2020.

Kurt Shuster, Samuel Humeau, Hexiang Hu, Antoine Bordes, and Jason Weston. Engaging image captioning via personality. In *Proceedings of the IEEE/CVF Conference on Computer Vision and Pattern Recognition*, pp. 12516–12526, 2019.

Simon Stepputtis, Joseph Campbell, Mariano Phielipp, Stefan Lee, Chitta Baral, and Heni Ben Amor. Language-conditioned imitation learning for robot manipulation tasks. *Neurips*, 2020.

Yixuan Su, Tian Lan, Huayang Li, Jialu Xu, Yan Wang, and Deng Cai. Pandagpt: One model to instruction-follow them all. *arXiv preprint arXiv:2305.16355*, 2023.

Alane Suhr, Mike Lewis, James Yeh, and Yoav Artzi. A corpus of natural language for visual reasoning. In *Proceedings of the 55th Annual Meeting of the Association for Computational Linguistics (Volume 2: Short Papers)*, pp. 217–223, 2017.

Alane Suhr, Stephanie Zhou, Ally Zhang, Iris Zhang, Huajun Bai, and Yoav Artzi. A corpus for reasoning about natural language grounded in photographs. *arXiv preprint arXiv:1811.00491*, 2018.

Yansong Tang, Dajun Ding, Yongming Rao, Yu Zheng, Danyang Zhang, Lili Zhao, Jiwen Lu, and Jie Zhou. Coin: A large-scale dataset for comprehensive instructional video analysis. In *Proceedings of the IEEE/CVF Conference on Computer Vision and Pattern Recognition*, pp. 1207–1216, 2019.

Ming Tao, Hao Tang, Songsong Wu, Nicu Sebe, Xiao-Yuan Jing, Fei Wu, and Bingkun Bao. Df-gan: Deep fusion generative adversarial networks for text-to-image synthesis. *arXiv preprint arXiv:2008.05865*, 2020.

Makarand Tapaswi, Yukun Zhu, Rainer Stiefelhagen, Antonio Torralba, Raquel Urtasun, and Sanja Fidler. Movieqa: Understanding stories in movies through question-answering. In *Proceedings of the IEEE conference on computer vision and pattern recognition*, pp. 4631–4640, 2016.

Jesse Thomason, Michael Murray, Maya Cakmak, and Luke Zettlemoyer. Vision-and-dialog navigation. In *Conference on Robot Learning*, pp. 394–406. PMLR, 2020.

Atousa Torabi, Christopher Pal, Hugo Larochelle, and Aaron Courville. Using descriptive video services to create a large data source for video annotation research. *arXiv preprint arXiv:1503.01070*, 2015.

Ashish Vaswani, Noam Shazeer, Niki Parmar, Jakob Uszkoreit, Llion Jones, Aidan N Gomez, Lukasz Kaiser, and Illia Polosukhin. Attention is all you need. *arXiv preprint arXiv:1706.03762*, 2017.

Hoa Trong Vu, Claudio Greco, Aliia Erofeeva, Somayeh Jafaritazehjan, Guido Linders, Marc Tanti, Alberto Testoni, Raffaella Bernardi, and Albert Gatt. Grounded textual entailment. *arXiv preprint arXiv:1806.05645*, 2018.

Teng Wang, Jinrui Zhang, Junjie Fei, Yixiao Ge, Hao Zheng, Yunlong Tang, Zhe Li, Mingqi Gao, Shanshan Zhao, Ying Shan, et al. Caption anything: Interactive image description with diverse multimodal controls. *arXiv preprint arXiv:2305.02677*, 2023.

Chenfei Wu, Jian Liang, Lei Ji, Fan Yang, Yuejian Fang, Daxin Jiang, and Nan Duan. N\" uwa: Visual synthesis pre-training for neural visual world creation. *arXiv preprint arXiv:2111.12417*, 2021.

Weihao Xia, Yujiu Yang, Jing-Hao Xue, and Baoyuan Wu. Tedigan: Text-guided diverse face image generation and manipulation. In *Proceedings of the IEEE/CVF conference on computer vision and pattern recognition*, pp. 2256–2265, 2021.

Ning Xie, Farley Lai, Derek Doran, and Asim Kadav. Visual entailment: A novel task for fine-grained image understanding. *arXiv preprint arXiv:1901.06706*, 2019.

Jun Xu, Tao Mei, Ting Yao, and Yong Rui. Msr-vtt: A large video description dataset for bridging video and language. In *Proceedings of the IEEE conference on computer vision and pattern recognition*, pp. 5288–5296, 2016.

Guangyu Robert Yang, Igor Ganichev, Xiao-Jing Wang, Jonathon Shlens, and David Sussillo. A dataset and architecture for visual reasoning with a working memory. In *Proceedings of the European Conference on Computer Vision (ECCV)*, pp. 714–731, 2018.

Rui Yang, Lin Song, Yanwei Li, Sijie Zhao, Yixiao Ge, Xiu Li, and Ying Shan. Gpt4tools: Teaching large language model to use tools via self-instruction. *arXiv preprint arXiv:2305.18752*, 2023a.

Zhengyuan Yang, Linjie Li, Jianfeng Wang, Kevin Lin, Ehsan Azarnasab, Faisal Ahmed, Zicheng Liu, Ce Liu, Michael Zeng, and Lijuan Wang. Mm-react: Prompting chatgpt for multimodal reasoning and action. *arXiv preprint arXiv:2303.11381*, 2023b.

Yuya Yoshikawa, Yutaro Shigeto, and Akikazu Takeuchi. Stair captions: Constructing a large-scale japanese image caption dataset. *arXiv preprint arXiv:1705.00823*, 2017.

Peter Young, Alice Lai, Micah Hodosh, and Julia Hockenmaier. From image descriptions to visual denotations: New similarity metrics for semantic inference over event descriptions. *Transactions of the Association for Computational Linguistics*, 2:67–78, 2014.

Oğuz Kaan Yüksel, Enis Simsar, Ezgi Gülperi Er, and Pinar Yanardag. Latentclr: A contrastive learning approach for unsupervised discovery of interpretable directions. *arXiv preprint arXiv:2104.00820*, 2021.

Rowan Zellers, Yonatan Bisk, Ali Farhadi, and Yejin Choi. From recognition to cognition: Visual commonsense reasoning. In *Proceedings of the IEEE/CVF Conference on Computer Vision and Pattern Recognition*, pp. 6720–6731, 2019.

Kuo-Hao Zeng, Tseng-Hung Chen, Juan Carlos Niebles, and Min Sun. Generation for user generated videos. In *European conference on computer vision*, pp. 609–625. Springer, 2016.

Han Zhang, Tao Xu, Hongsheng Li, Shaoting Zhang, Xiaogang Wang, Xiaolei Huang, and Dimitris N Metaxas. Stackgan: Text to photo-realistic image synthesis with stacked generative adversarial networks. In *Proceedings of the IEEE international conference on computer vision*, pp. 5907–5915, 2017.

Han Zhang, Tao Xu, Hongsheng Li, Shaoting Zhang, Xiaogang Wang, Xiaolei Huang, and Dimitris N Metaxas. Stackgan++: Realistic image synthesis with stacked generative adversarial networks. *IEEE transactions on pattern analysis and machine intelligence*, 41(8):1947–1962, 2018.

Han Zhang, Jing Yu Koh, Jason Baldridge, Honglak Lee, and Yinfei Yang. Cross-modal contrastive learning for text-to-image generation. In *Proceedings of the IEEE/CVF conference on computer vision and pattern recognition*, pp. 833–842, 2021.

Lin Zhang, Lei Zhang, Xuanqin Mou, and David Zhang. Fsim: A feature similarity index for image quality assessment. *IEEE transactions on Image Processing*, 20(8):2378–2386, 2011.

Tianjun Zhang, Yi Zhang, Vibhav Vineet, Neel Joshi, and Xin Wang. Controllable text-to-image generation with gpt-4. *arXiv preprint arXiv:2305.18583*, 2023.

Zhiqiang Zhang, Wenxin Yu, Jinjia Zhou, Xuewen Zhang, Ning Jiang, Gang He, and Zhuo Yang. Customizable gan: A method for image synthesis of human controllable. *IEEE Access*, 8:108004–108017, 2020.

Zijia Zhao, Longteng Guo, Tongtian Yue, Sihan Chen, Shuai Shao, Xinxin Zhu, Zehuan Yuan, and Jing Liu. Chatbridge: Bridging modalities with large language model as a language catalyst. *arXiv preprint arXiv:2305.16103*, 2023.

Luowei Zhou, Chenliang Xu, and Jason Corso. Towards automatic learning of procedures from web instructional videos. In *Proceedings of the AAAI Conference on Artificial Intelligence*, volume 32, 2018.

Yimin Zhou, Yiwei Sun, and Vasant Honavar. Improving image captioning by leveraging knowledge graphs. In *2019 IEEE winter conference on applications of computer vision (WACV)*, pp. 283–293. IEEE, 2019.

Deyao Zhu, Jun Chen, Xiaoqian Shen, Xiang Li, and Mohamed Elhoseiny. Minigpt-4: Enhancing vision-language understanding with advanced large language models. *arXiv preprint arXiv:2304.10592*, 2023.

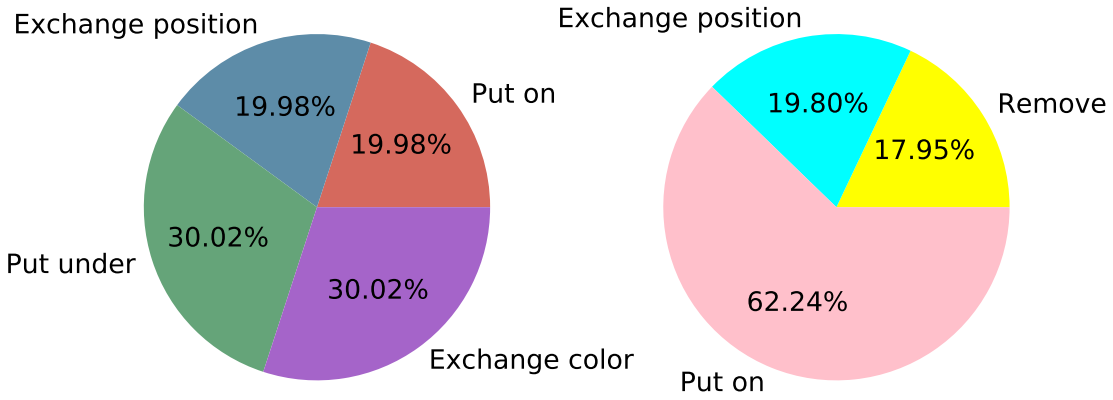

Figure A1: The distribution of different actions on CLEVR-ATVC and Fruit-ATVC datasets.

A Additional Data Details

This section provides further information about the data used in our research. We begin by introducing the format of the annotation files for our datasets. Additionally, we present a wider range of example images from the Fruit-ATVC dataset to highlight the diversity of collection scenes. Lastly, we provide a summary of statistics regarding the various actions found in the datasets.

A.1 Annotation File Format

We describe the format of the annotation files for both the CLEVR-ATVC and Fruit-ATVC datasets. Listings 1 and 2 demonstrate the consistent structure of the annotation files, with the primary distinction being the inclusion of detailed 2D and 3D coordinate locations of objects in the CLEVR-ATVC dataset. Figure B2 provides a visual representation of the bounding boxes in the CLEVR-ATVC dataset. It is worth noting that we anticipate the potential use of this dataset for other related tasks, such as compositional visual reasoning. While we have previously introduced the main structure of the annotation files in the main paper, we now aim to provide additional details.

The annotation files begin by providing a summary of the dataset contributors, timestamp, project link, version, and license information. This introductory section ensures comprehensive documentation and proper attribution. Following this, the annotation files include the categories of objects present in the dataset, along with associated object adjectives, actions, and other relevant information.

The "images" section contains all the necessary information about the visual inputs. This includes the image index, filename, link, the number of objects in the image, and detailed descriptions of each object present. Each object is listed under the "objects" child list, accompanied by specific properties such as index, category index, and bounding box coordinates.

The text-based queries (Q) and textual feedback (A) are included in the "questions" section of the annotation files. The answer types are indicated by numbers ranging from 0 to 2. Specifically, a value of 0, 1, or 2 represents an instruction that cannot be executed, an instruction that can be executed, or a prohibited instruction, respectively. If the action type is 0 or 2, the subsequent "actions" list in the "recreations" section will be empty. Notably, the CLEVR-ATVC dataset provides additional information regarding any changes in the color or position of an object after a displacement or property modification.

A.2 Diversity of Fruit-ATVC

The following Figure B3 shows the diversity of collection scenes on Fruit-ATVC dataset. The image resolution is average 2700×2700, and the images were taken with different categories of mobile phones, including iphone, huawei, xiaomi, etc. We would like to emphasize that the image quality of this dataset is very high, which results in the size of the original Fruit-ATVC is 168 GB. In addition, Moreover, the background of data

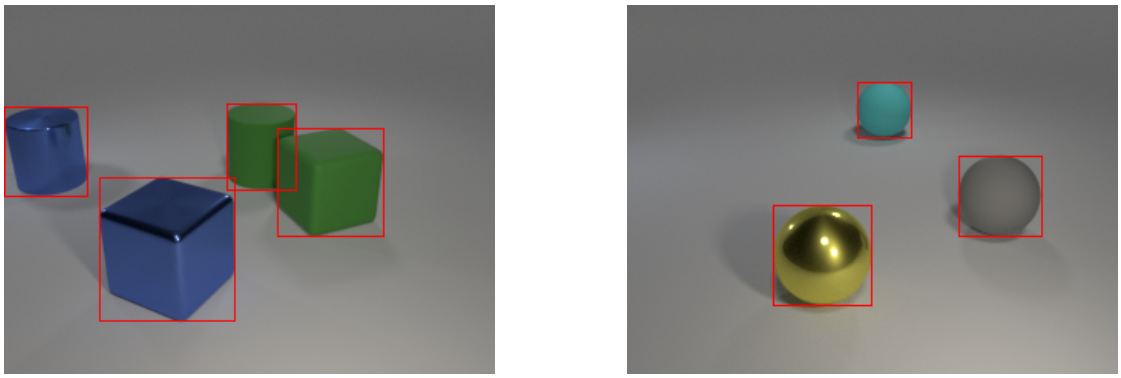

Figure B2: The visualization of bounding boxes in the CLEVR-ATVC dataset.

collection, fruit categories and container types are also very diverse. We believe this dataset can also be used for other image generation tasks. The Figure A1 illustrates the distribution of different actions on our constructed datasets.

B Human Evaluation Experiments

This section presents examples of the interfaces utilized for facilitating human evaluation. During the evaluation phase, the visual input, text-based query, re-created image, answer, and ground truths for re-creation and textual feedback are automatically imported into the corresponding sections of the auxiliary tool. Evaluators are then only required to assign scores to the respective results and save them. Subsequently, we calculate the final score of the model based on the saved results.

As detailed in the main paper, we assigned the same results to different evaluators, with each evaluator providing identical scores for the experimental outcomes. The aforementioned experiments demonstrate that the auxiliary tools we have designed not only significantly reduce the evaluation time required but also ensure the accuracy and reliability of the widely used human evaluation process.

Figure B3: The example images of Fruit-ATVC dataset show the diversity of collection scenes.

Listing 1: The format of annotation file on CLEVR-ATVC dataset.


```
{
  "contributor": "Anonymous",
  "data_created": "2023",
  "url": "Anonymous",
  "description": "CLEVR-ATVC Dataset",
  "vertion": "1.0",
  "licenses": {
    "id": "1",
    "url": "Nnone",
    "name": "Creative Commons Attribution (CC-BY 4.0)",
  },
  "categories": ["cube, cylinder, sphere"],
  "sizes": ["small, large"],
  "colors": ["gray, red, blue, green, brown, purple, cyan, yellow"],
  "material": ["rubber, metal"],
  "actions": ["put on top, put under, exchange position, exchange color"],
  "images": [
        {
        "image_idx": "0000001",
        "image_filename": "521100_03_000011.png",
        "id": "521100_03_000011",
        "object_number": 3,
        "atvc_url": "http://images.atvcdata.org/clevratvc/train2023/V/521100_03_000011.png
        "data_created": "2023-04-27 00:17:14",
        "objects": [
            {
            "index": 0,
            "category_id": 0,
            "size_id": 1,
            "color_id": 3,
            "bbox": [29, 62, 81, 116],
            "3d_coords": [-2.96856045, -1.99158716, 0.6999999],
            "material_id": 1},
            {...},
            {...},
                    ]
        },
    ]
  "questions": [
        {
        "question_idx": "0000001",
        "question_id": "521100_03_000011",
        "question_number": 10,
        "ques": [
            {
            "ques_id": 0,
            "ques_idx": 1,
            "id": "521100_03_000011_0_01",
            "type": 1,
            "Q": ["Please put the cylinder on top of the cube."],
            "A": ["No problem."]
            },
        ]
```

```
    "recreations": [
        {
        "rec_idx": "0000001",
        "rec_id": "521100_03_000011",
        "rec_num": 10,
        "actions": [
            {
            "actions_id": 0,
            "actions_idx": 1,
            "rec_filename": "521100_03_000011_0_01.png",
            "object_number": 3,
            "atvc_url": "http://images.atvcdata.org/clevratvc/train2023/M/521100_03_000011_
            "date_created": "2023-04-27 00:17:59",
            "objects": [
            {},
            {},
            {
            "index": 2,
            "category_id": 1,
            "size_id": 0,
            "color_id": 1,
            "bbox": [39, 45, 65, 72],
            "3d_coords": [-2.96856045, -1.99158716, 1.75],
            "material_id": 0}
                        ]
            },
        ]
}
```

Listing 2: The format of annotation file on Fruit-ATVC dataset.


```
{
  "contributor": "Anonymous",
  "data_created": "2023",
  "url": "Anonymous",
  "description": "Fruit-ATVC Dataset",
  "vertion": "1.0",
  "licenses": {
    "id": "1",
    "url": "Nnone",
    "name": "Creative Commons Attribution (CC-BY 4.0)",
  },
  "fruits": ["apple, pear, cocount, orange, banana, kiwi, mango, avocado, lemon, pitaya"],
  "containers": ["plate, bowl, bottle"],
  "actions": ["put in, exchange position, remove"],
  "images": [
        {
        "image_idx": "0000001",
        "image_filename": "0000001.png",
        "id": "0000001",
        "fruit_number": 3,
        "container_number": 1,
        "atvc_url": "http://images.atvcdata.org/fruitatvc/train2023/V/0000001.png",
        "data_created": "2023-04-27 00:10:11",
        "fruits": [
                {
                    "index": 0,
                    "category_id": 0
                }
                {
                    "index": 1,
                    "category_id": 6
                }
                {
                    "index": 2,
                    "category_id": 8
                }
            ],
        "containers": [
                {
                    "index": 0,
                    "category_id": 2
                }
            ],
        },
    ]
  "questions": [
        {
        "question_idx": "0000001",
        "question_id": "0000001",
        "question_number": 3,
        "ques": [
            {
            "ques_id": 0,
```

```
            "ques_idx": 1,
            "id": "0000001_0_01",
            "type": 1,
            "Q": ["Please put the kiwi in the plate."],
            "A": ["No problem."]
            },
        ]
    "recreations": [
        {
        "rec_idx": "0000001",
        "rec_id": "0000001",
        "rec_num": 3,
        "actions": [
            {
            "actions_id": 0,
            "actions_idx": 1,
            "rec_filename": "0000001_0_01.png",
            "fruit_number": 3,
            "container_number": 1,
            "atvc_url": "http://images.atvcdata.org/fruitatvc/train2023/M/0000001_0_01.png
            "date_created": "2023-04-27 00:10:18",
            },
        ]
}
```

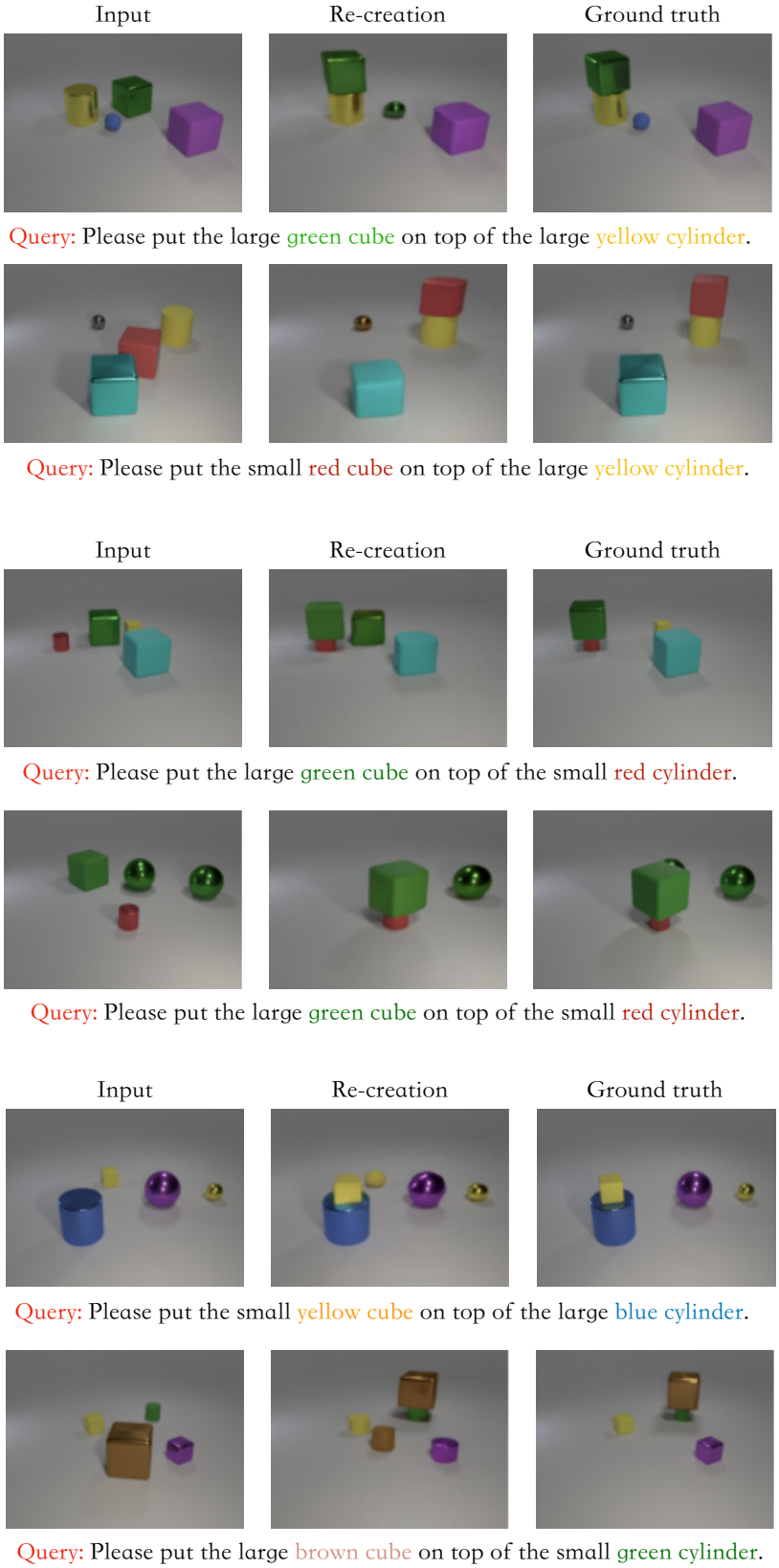

Figure B4: More results are to show why VQGAN-based image encoder performs worse on image re-creation.

Input | Re-creation | Ground truth

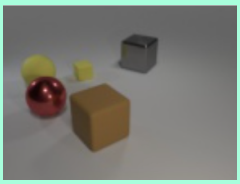

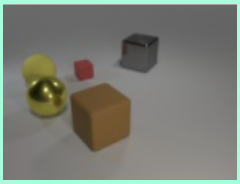

Query: Please exchange the color of the small yellow rubber cube and the large red metal sphere.

Answer: No problem.

Ground truth: No problem.

Human Evaluation

1. Please rate the visual re-creation?

● A: 1 ○ B: 0.5 ○ C: 0

2. Please rate the type of answer?

● 1 ○ 0

3. Please rate the explanation of answer?

● 1 ○ 0

4. What is the score for textual feedback? [1.0]

5. What is the full-match score? [1.0]

Input | Re-creation | Ground truth

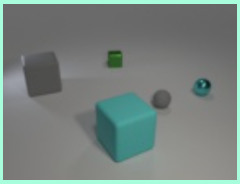

Query: Please put the large gray metal cylinder under the small yellow rubber cylinder.

Answer: This action cannot be done. Because there is no large gray metal cylinder and no small yellow rubber cylinder.

Ground truth: This action cannot be done. Because there is no large gray metal cylinder and no small yellow rubber cylinder.

Human Evaluation

1. Please rate the visual re-creation?

● A: 1 ○ B: 0.5 ○ C: 0

2. Please rate the type of answer?

● 1 ○ 0

3. Please rate the explanation of answer?

● 1 ○ 0

4. What is the score for textual feedback? [1.0]

5. What is the full-match score? [1.0]

Input | Re-creation | Ground truth

Query: Please put the large tray metal cube on top of the large blue metal sphere.

Answer: This action is forbidden. Because you cannot put an object on top of the sphere, and there is no large gray metal cube and no large blue metal sphere.

Ground truth: This action is forbidden. Because you cannot put an object on top of the sphere, and there is no large gray metal cube and no large blue metal sphere.

Human Evaluation

1. Please rate the visual re-creation?

● A: 1 ○ B: 0.5 ○ C: 0

2. Please rate the type of answer?

● 1 ○ 0

3. Please rate the explanation of answer?

● 1 ○ 0

4. What is the score for for textual feedback? [1.0]

5. What is the full-match score? [1.0]

Input | Re-creation | Ground truth

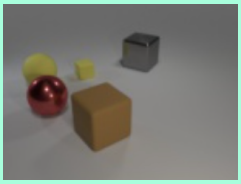

Query: Please put the large red metal sphere under the small yellow rubber cube.

Answer: This action is forbidden. Because you cannot put the sphere under an object, and there is no large red metal sphere and no small yellow rubber cube.

Ground truth: This action is forbidden. Because you cannot put the sphere under an object.

Human Evaluation

1. Please rate the visual re-creation?

● A: 1 ○ B: 0.5 ○ C: 0

2. Please rate the type of answer?

● 1 ○ 0

3. Please rate the explanation of answer?

○ 1 ● 0

4. What is the score for for textual feedback? [0.5]

5. What is the full-match score? [0.75]

Input | Re-creation | Ground truth

Query: Please put the small yellow metal sphere under the large red metal cube.

Answer: This action is forbidden. Because you cannot put the sphere under an object, and there is no small yellow metal sphere and no small red metal cube.

Ground truth: This action is forbidden. Because you cannot put the sphere under an object, and there is no small yellow metal sphere and no large red metal cube.

Human Evaluation

1. Please rate the visual re-creation?

● A: 1 ○ B: 0.5 ○ C: 0

2. Please rate the type of answer?

● 1 ○ 0

3. Please rate the explanation of answer?

○ 1 ● 0

4. What is the score for for textual feedback? [0.5]

5. What is the full-match score? [0.75]

Input | Re-creation | Ground truth

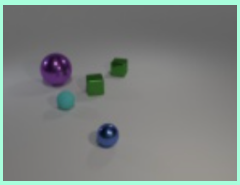

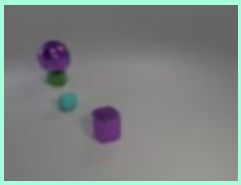

Query: Please put the small green metal cube under the large purple metal sphere.

Answer: No problem.

Ground truth: No problem

Human Evaluation

1. Please rate the visual re-creation?

○ A: 1 ● B: 0.5 ○ C: 0

2. Please rate the type of answer?

● 1 ○ 0

3. Please rate the explanation of answer?

● 1 ○ 0

4. What is the score for for textual feedback? [1.0]

5. What is the full-match score? [0.75]

Input | Re-creation | Ground truth

Query: Please put the large purple metal sphere on top of the large purple metal cylinder.

Answer: This action is forbidden. Because you cannot put the sphere under an object.

Ground truth: No problem.

Human Evaluation

1. Please rate the visual re-creation?

   ○ A: 1 ○ B: 0.5 ● C: 0

2. Please rate the type of answer?

   ○ 1 ● 0

3. Please rate the explanation of answer?

   ○ 1 ● 0

4. What is the score for for textual feedback? [0]

5. What is the full-match score? [0]

Input | Re-creation | Ground truth

Query: Please exchange the position of the large yellow metal cube and the large green metal cylinder.

Answer: No problem.

Ground truth: This action cannot be done. Because there is no large yellow metal cube and no large metal cylinder.

Human Evaluation

1. Please rate the visual re-creation?

   ○ A: 1 ○ B: 0.5 ● C: 0

2. Please rate the type of answer?

   ○ 1 ● 0

3. Please rate the explanation of answer?

   ○ 1 ● 0

4. What is the score for for textual feedback? [0]

5. What is the full-match score? [0]